

Received:
29 December 2013

Revised:
9 June 2014

Accepted:
3 July 2014

doi: 10.1259/bjr.20140011

Cite this article as:

Moritani T, Kim J, Capizzano AA, Kirby P, Kademian J, Sato Y. Pyogenic and non-pyogenic spinal infections: emphasis on diffusion-weighted imaging for the detection of abscesses and pus collections. *Br J Radiol* 2014;87:20140011.

REVIEW ARTICLE

Pyogenic and non-pyogenic spinal infections: emphasis on diffusion-weighted imaging for the detection of abscesses and pus collections

¹T MORITANI, MD, PhD, ¹J KIM, MD, ¹A A CAPIZZANO, MD, ²P KIRBY, MD, ¹J KADEMIAN, MD and ¹Y SATO, MD, PhD

¹Department of Radiology, University of Iowa Hospitals and Clinics, Iowa City, IA, USA

²Department of Pathology, University of Iowa Hospitals and Clinics, Iowa City, IA, USA

Address correspondence to: Professor Toshio Moritani

E-mail: toshio-moritani@uiowa.edu

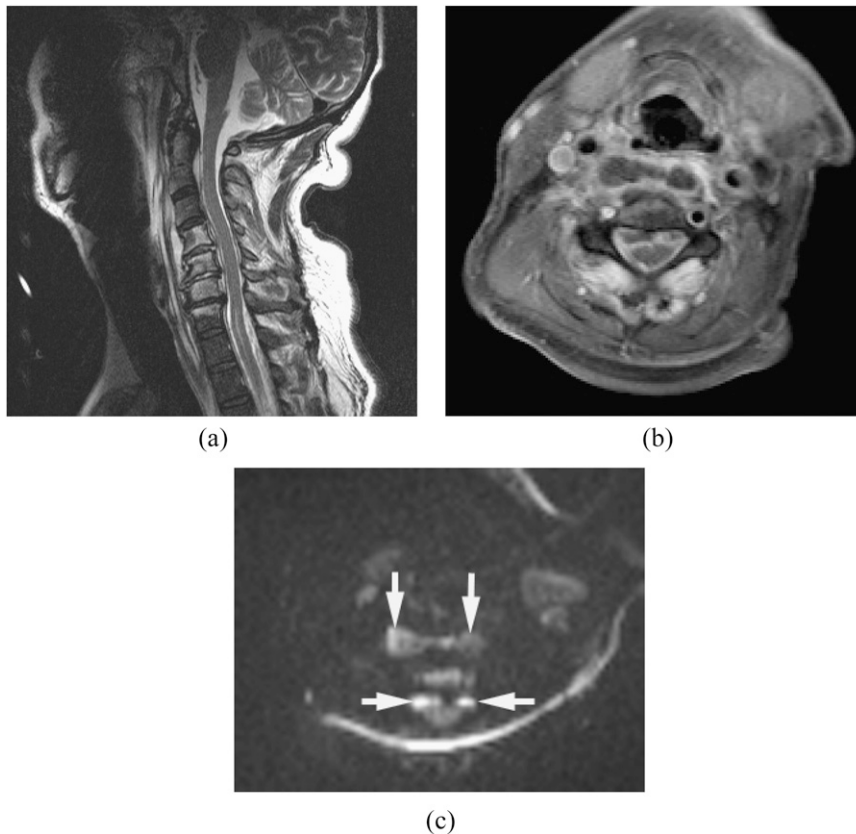
ABSTRACT

The incidence of spinal infections has increased in the past two decades, owing to the increasing number of elderly patients, immunocompromised conditions, spinal surgery and instrumentation, vascular access and intravenous drug use. Conventional MRI is the gold standard for diagnostic imaging; however, there are still a significant number of misdiagnosed cases. Diffusion-weighted imaging (DWI) with a *b*-value of 1000 and apparent diffusion coefficient (ADC) maps provide early and accurate detection of abscess and pus collection. Pyogenic infections are classified into four types of extension based on MRI and DWI findings: (1) epidural/paraspinal abscess with spondylodiscitis, (2) epidural/paraspinal abscess with facet joint infection, (3) epidural/paraspinal abscess without concomitant spondylodiscitis or facet joint infection and (4) intradural abscess (subdural abscess, purulent meningitis and spinal cord abscess). DWI easily detects abscesses and demonstrates the extension, multiplicity and remote disseminated infection. DWI is often a key image in the differential diagnosis. Important differential diagnoses include epidural, subdural or subarachnoid haemorrhage, cerebrospinal fluid leak, disc herniation, synovial cyst, granulation tissue, intra- or extradural tumour and post-surgical fluid collections. DWI and the ADC values are affected by susceptibility artefacts, incomplete fat suppression and volume-averaging artefacts. Recognition of artefacts is essential when interpreting DWI of spinal and paraspinal infections. DWI is not only useful for the diagnosis but also for the treatment planning of pyogenic and non-pyogenic spinal infections.

Spinal and paraspinal infections include vertebral osteomyelitis, spondylodiscitis, infectious facet arthropathy, epidural infections, meningitis, myelitis and infections of paraspinal soft tissue and musculature. Evidence of spinal infections has been discovered in the remains of pre-historic humans from 7000 BC.¹ The incidence has increased in the past two decades, owing to the rising number of elderly patients, immunocompromised conditions, spinal surgery and instrumentation, vascular access and intravenous drug use.¹⁻⁴ Despite advances in medical knowledge, imaging modalities and surgical interventions, the diagnosis of this entity is still challenging since the clinical features can be subtle and misleading. MRI including post-contrast studies is the gold standard for diagnostic imaging. However, although MRI has relatively high diagnostic sensitivity, specificity and accuracy, there are still a significant number of challenging cases. In such cases, diagnostic delays and suboptimal management can result in irreversible paralysis, critical sepsis and even death.

Diffusion-weighted imaging (DWI) has proven to be a useful tool for the diagnosis of a variety of intracranial infections especially in the detection of brain abscesses and pus collections, which encompass subdural and epidural empyema, purulent meningitis and ventriculitis.⁵⁻⁸ Therefore, DWI is considered to be useful in the evaluation of the extension of abscesses and pus collections in spinal and paraspinal infections.^{9,10} It is often a key image in the differential diagnosis. In this article, we demonstrate DWI findings in pyogenic and non-pyogenic spinal infections involving epidural/subdural spaces, leptomeninges, spinal cord, paraspinal soft tissue and iliopsoas muscle as well as other disseminated infections. We also illustrate and discuss the differential diagnosis and imaging pitfalls. Important differential diagnoses include epidural, subdural or subarachnoid haemorrhage, cerebrospinal fluid (CSF) leak, disc herniation, synovial cyst, granulation tissue, intra- or extradural tumour and post-surgical fluid collections.

Figure 1. Epidural abscess and pre-vertebral/retropharyngeal abscesses with spondylodiscitis. Methicillin-resistant *Staphylococcus aureus* was proven by surgical drainage. (a) Sagittal T_2 weighted image reveals high signal intensities in the disc and vertebral bodies from C4 through C6, with epidural, pre-vertebral and retropharyngeal abscesses. (b) Axial post-contrast T_1 weighted image with fat saturation shows multiple ring enhancing lesions. (c) Diffusion-weighted imaging clearly demonstrates the extension of the abscesses (arrows). Incomplete fat saturation artefacts are seen in the subcutaneous fat.



MRI AND DIFFUSION-WEIGHTED IMAGING

MRI is the diagnostic imaging modality of choice for evaluating spinal and paraspinal infections. MRI plays an essential role in the decision-making process concerning conservative *vs* surgical management and monitoring the effect of treatment. MRI has high diagnostic sensitivity, specificity and accuracy of >90%.^{1,3,4,11–15} However, on conventional MRI even with gadolinium enhancement, it is occasionally difficult to differentiate abscess/pus collection from other pathologies such as post-surgical fluid collection, cystic/necrotic tumour, haematoma, CSF leak and unusual patterns of degenerative disc and facet joint changes.

DWI with $b = 0$ and 1000 s mm^{-2} and the apparent diffusion coefficient (ADC) map have routinely been performed for the diagnosis of intracranial infections especially in the detection of brain abscesses and pus collections.^{5–8} Abscesses and pus collections are viscous fluid containing cellular debris and necrosis with dead or viable neutrophils causing the restriction of water molecule movement that demonstrates hyperintensity on DWI. Therefore, DWI is potentially a very useful tool in diagnosing spinal and paraspinal infections.^{9,10} If gadolinium contrast cannot be performed owing to significant renal failure, especially in diabetic patients, or if other MR sequences are suboptimal in delineating abscesses because of motion artefacts, DWI is crucial. We use

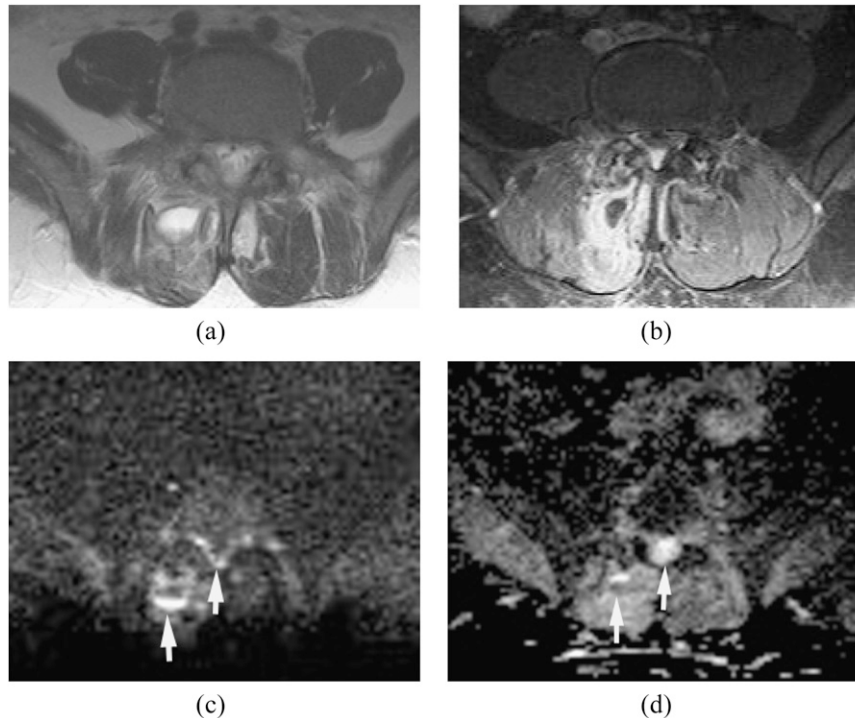
spin-echo-type echoplanar DWI, which allows a fast sequence with less motion artefacts. For the appropriate detection and evaluation of abscesses and pus collections, DWI is performed with $b = 0$ and 1000 s mm^{-2} and the ADC map. Parallel imaging factor 2 is used to reduce distortion in images.

DWI demonstrates the extension and multiplicity of abscesses, even if small, in any spinal or paraspinal area. While not previously clearly described, we believe it is useful not only for the early and accurate diagnosis of abscess/pus collections but also for defining treatment plan, site selection for biopsy or planning for surgical drainage.

PYOGENIC INFECTION

About two-thirds of causative organisms are *Staphylococcus aureus*, including methicillin-resistant *S. aureus* (MRSA) and methicillin-susceptible *S. aureus*.^{1–4,16} MRSA is increasingly seen in both healthcare-associated and community-acquired infections and is associated with a higher complication rate and prolonged treatment courses.^{17,18} Other less common infectious agents include *S. epidermidis* (spine procedures), *Streptococcus* and *Enterococcus* (coexisting infective endocarditis), *Escherichia coli* (urinary tract infection), *Pseudomonas aeruginosa* (intravenous-drug abuse), *Salmonella* (sickle cell disease), anaerobic bacteria (abdominal and pelvic infections and gastrointestinal procedures),

Figure 2. Epidural and paraspinal abscesses with septic facet joint infection. Methicillin-susceptible *Staphylococcus aureus* was proven by surgical drainage. (a) Axial T_2 weighted image reveals high signal intensity in the right spinous muscle at L4-L5. It is difficult to detect small epidural abscesses. (b) Axial post-contrast T_1 weighted image with fat saturation shows the paraspinal abscess and epidural enhancement with associated facet joint infection. (c, d) Diffusion-weighted imaging (c) demonstrates the paraspinal abscess and small epidural abscesses as hyperintense with partially increased apparent diffusion coefficient values (d) likely due to dilution by exudates and/or partial volume artefacts (arrows).



Mycobacterium tuberculosis, non-tuberculous mycobacteria, nocardia, actinomycetes and *Brucella* (endemic areas).

Organisms infect the spinal and paraspinal structures via two routes: haematogenous and non-haematogenous.¹⁻⁴ In approximately half of spinal infections, the source is haematogenous dissemination, one-third is contiguous spread (surgical intervention, trauma and direct inoculation) and in the remaining cases, the source of infection is unidentified. The dense region of arterial and venous channel networks is confined to bony end plates in adults, whereas in children, hyaline cartilage contains perforating vessels until 7 years of age with concomitant increased susceptibility to primary discitis.¹⁹⁻²¹ However, disc revascularization can occur with degenerative disc changes and spondyloarthropathy.⁴ Organisms that produce proteolytic enzymes quickly spread into the end plate and destroy the disc substance and then extend into the epidural or paraspinal spaces.⁴ The valveless Batson's venous plexus may contribute to early extension and seeding of spinal and paraspinal infections.^{4,14,22-25} The terminal branches of the same artery may supply the spinal and paraspinal area. Therefore, one site of spinal and paraspinal infections can extend locally or can disseminate hematogenously to other spinal/paraspinal areas or remote areas of the body.

The clinical features and laboratory findings of spinal infections can be subtle and misleading. Local back pain and fever are

common but not always present. Elevated white blood cell count is detected in two-thirds of the cases. Elevated C-reactive protein and erythrocyte sedimentation rate are useful screening laboratory tests. Mortality rates have been reported in the range of 2-20% for vertebral osteomyelitis and around 5% for epidural abscess, whereas in the pre-antibiotic era, they were 25-70%.^{2-4,16,23} Paraplegia or tetraplegia occur in 1% of patients especially with cervical and thoracic spine infections.

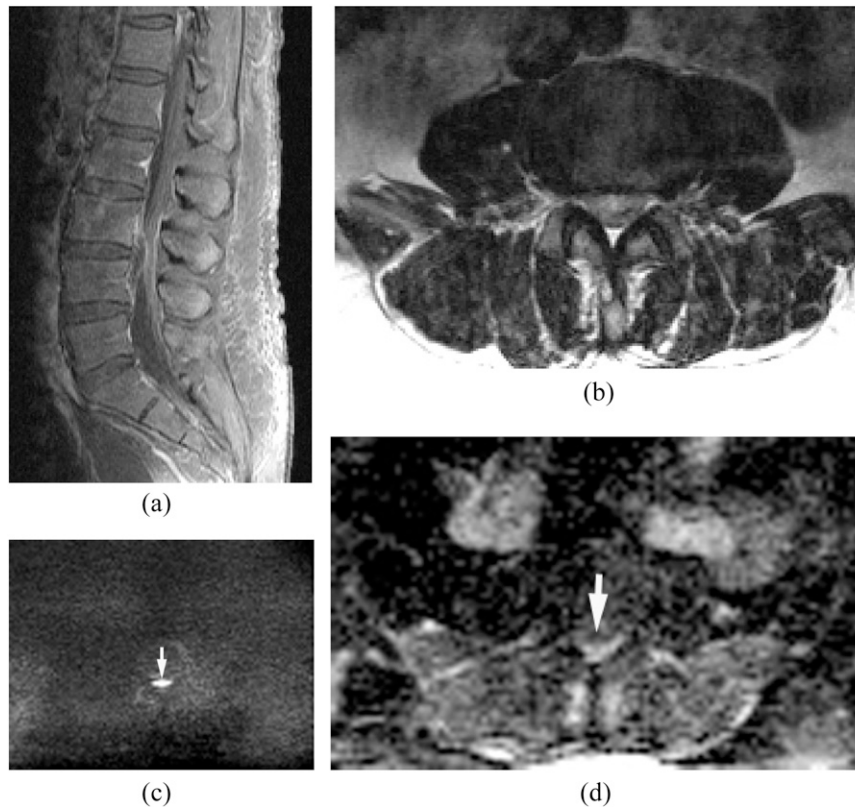
PATTERNS OF EXTENSION OF PYOGENIC ABSCESS AND PUS COLLECTION

We classified pyogenic spinal and paraspinal infections based on the pattern of extension. Recognition of these patterns is helpful to identify abscess/pus collection and other spinal infections on MRI and DWI:

- (1) epidural/paraspinal abscess with spondylodiscitis
- (2) epidural/paraspinal abscess with facet joint infection
- (3) epidural/paraspinal abscess without concomitant spondylodiscitis or facet joint infection
- (4) intradural abscess (subdural abscess, purulent meningitis and spinal cord abscess).

Epidural/paraspinal abscess with spondylodiscitis
Epidural/paraspinal abscess associated with spondylodiscitis is the most common pattern of extension. Pyogenic spondylodiscitis (osteomyelitis/discitis) commonly occurs in the lumbar spine. Cervical spondylitis can progress anteriorly causing

Figure 3. Isolated small ventral epidural abscess mimicking a disc herniation. *Streptococcus milleri* was proven by surgical drainage. (a) Sagittal post-contrast T_1 weighted image shows a lesion at L3/4 ventrally with peripheral enhancement. There is no abnormal enhancement in the adjacent disc and vertebral body. (b) Axial T_2 weighted image shows slightly hyperintense lesion on T_2 weighted image. (c, d) Diffusion-weighted imaging (c) early reveals the lesion as hyperintense with decreased apparent diffusion coefficient (d) consistent with an epidural abscess (arrows).



retropharyngeal abscess and inferiorly causing mediastinitis. Thoracic spondylitis can cause mediastinitis, empyema and pericarditis, while lumbar spondylitis causes peritonitis, subdiaphragmatic abscess and infection in the pelvis. Abscesses can also form within the vertebral body and disc.⁴

Multilevel involvement of vertebral bodies and discs can occur in pyogenic spinal infections but less commonly than in tuberculosis. Epidural abscess associated with discitis/osteomyelitis is often seen in the anterior part of the epidural space. Although epidural abscess usually extends over three to four vertebrae, it can involve the whole spine and is known as panspinal infection.^{2,26,27}

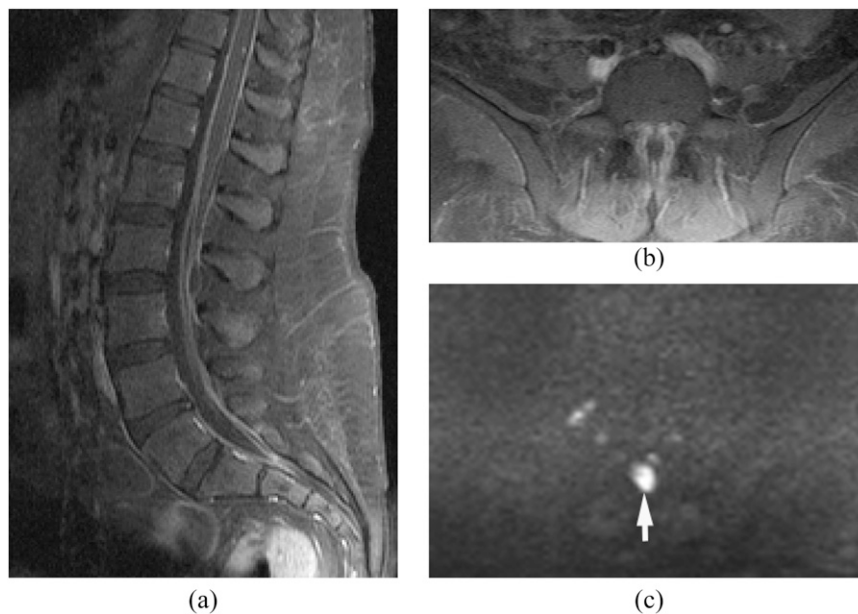
MRI findings of pyogenic spondylodiscitis include high signal on T_2 weighted images and low signal on T_1 weighted images with contrast enhancement. T_2 weighted images demonstrate spinal cord compression and abnormal cord signal.^{1,9,11,14,28,29} Gadolinium-enhanced T_1 weighted images with fat saturation can differentiate infection from post-surgical changes, and pus collection from granulation/phlegmon, based on the enhancement pattern.^{11,30,31} DWI is useful in the detection of small abscess or pus collection in the epidural space, paraspinal musculature, iliopsoas muscle, vertebral body and disc (Figure 1).

Epidural/paraspinal abscess with facet joint infection

Facet joint infection (septic arthritis) is rare but has increased recently, owing to the increase in the elderly population, immunocompromised patients and spine procedures.^{32–35} This is another important route of infection resulting in epidural/paraspinal abscesses. Facet joint infection is often haematogenous but also caused by epidural anaesthesia and spinal procedures. It is usually unilateral, and presents more acutely than does spondylodiscitis. It frequently involves the L4–L5 joints. Epidural abscess associated with facet joint infection tends to occur in the posterior part of the epidural space. Degenerative facet joints may constitute an increased risk for infection.³³ Infection of the facet joint often spreads contiguously to the epidural space and to the paraspinal musculature. Intradural extension associated with facet joint infection has also been reported.³⁶ If there is no evidence of spondylodiscitis, the facet joints should be evaluated very carefully.

The MRI findings of facet joint infection are sometimes very subtle and resemble degenerative joint disease. MRI shows swelling of the capsule and periarticular soft tissue of the facet joint. DWI is useful in the detection of small abscess or pus collection in the posterior paraspinal muscle adjacent to the facet joint (Figure 2).

Figure 4. Purulent meningitis after steroid epidural injection at an outside hospital. Methicillin-susceptible *Staphylococcus aureus* was proven in the cerebrospinal fluid (CSF). (a, b) Sagittal (a) and axial (b) post-contrast T_1 weighted image show extensive meningeal enhancement in the thecal sac. (c) Diffusion-weighted imaging demonstrates hyperintensity in the thecal sac consistent with purulent meningitis (arrow). Methicillin-resistant *Staphylococcus aureus* was proven in the CSF.



Epidural/paraspinal abscess without concomitant spondylodiscitis or facet joint infection

The route of this pattern of infection is variable: (1) isolated epidural or paraspinal abscess due to haematogenous spread, (2) direct extension from wound infection after surgery or trauma and (3) direct inoculation from spinal intervention such as epidural steroid injection or nerve block. Isolated epidural abscess is more commonly seen in the cervical spine.^{4,16} Isolated epidural abscess tends to occur posteriorly but can occur anteriorly. Diagnosis is often difficult clinically and radiologically. MRI with DWI is the key imaging technique in the diagnosis of isolated epidural abscess (Figure 3).

Intradural abscess (subdural abscess, purulent meningitis and spinal cord abscess)

Within the spinal canal, the epidural space is the most commonly affected but subdural involvement with meningitis and direct involvement of the spinal cord can occur.^{36–39} Intradural abscess is a rare entity but it is a neurosurgical emergency associated with high morbidity and mortality. Progressive neurological deficits, severe pain and fever suggest the diagnosis. Subdural abscess and purulent meningitis can be secondary to haematogenous spread, secondary infection after spine surgery and inoculation due to lumbar puncture, epidural steroid injection or nerve block (Figure 4).

Extension of bacterial meningitis with spinal dysraphism is also an important aetiology in children with this condition (Figure 5). MRI with DWI is very useful for the diagnosis of intradural abscesses.³⁹

MANAGEMENT

The mainstay of treatment of epidural and paraspinal abscesses is surgical decompression with drainage and long-term systemic

antibiotic treatment.^{2–4,16} Since paralysis lasting more than 24–36 h is unlikely to reverse, urgent decompressive laminectomy is indicated for epidural abscess. Antibiotic therapy must be guided by the results of blood, pus or biopsy tissue cultures. Several techniques have improved specimen acquisition, which include fine needle aspiration, percutaneous core biopsy and laparoscopic and open surgical biopsy.³ Pending the result of cultures, appropriate empirical antibiotic therapy should be administered. Diagnostic delays and suboptimal management can result in irreversible paralysis, worsening sepsis and death.

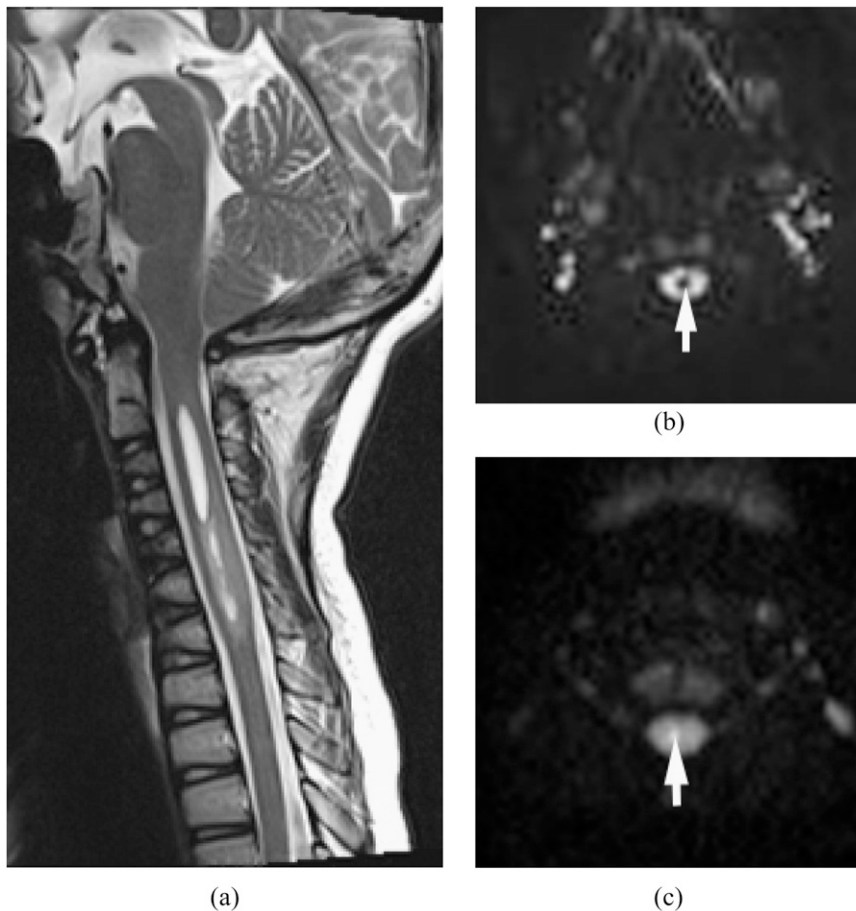
We believe DWI is very useful for defining treatment plan, site selection for biopsy or decision-making of surgical drainage.

NON-PYOGENIC INFECTION

Tuberculosis is the most common non-pyogenic infection.^{3,16,40,41} Reactivation of tuberculosis has increased with HIV infection, recent chemotherapy and concurrent steroid use and the use of anti-tumour necrosis factor agents (infliximab). Among the 30 million people currently affected with tuberculosis worldwide, 1–3% have skeletal involvement. Tuberculous spinal infections are more indolent than pyogenic spinal infection with a more gradual onset of symptoms over months to years. Since *M. tuberculosis* does not have proteolytic enzymes that allow it to spread into the disc, it spreads slowly and results in large paravertebral abscesses. The infection starts from the anterior subchondral region of the vertebral bodies or neural arch and often spreads under the anterior longitudinal ligament (subligamentous spread). Intervertebral discs are relatively preserved.

Tuberculosis is more common in the thoracic spine than in the lumbar spine.^{3,16} Multiple vertebral body involvement is

Figure 5. Spinal cord abscess with Chiari 1 malformation. (a) Sagittal T_2 weighted image shows a syrinx as hyperintense lesions from C2 through C6. (b, c) Diffusion-weighted imaging demonstrates hypointensity in the syrinx (b) and hyperintensity in the spinal cord abscess (arrow) (c).



common. Involvement of posterior elements of the spine and psoas abscess is another characteristic of tuberculosis. Evidence of pulmonary involvement is only seen in 50% of cases.

MRI typically demonstrates destruction of more than two consecutive vertebrae with relative sparing of the intervening disc and associated large paraspinal abscesses.^{3,16,40} Epidural infection can be seen. DWI usually shows restricted diffusion in the abscess (Figure 6). DWI can show partially hyper- and partially hypointense signal associated with high and low ADC values. The high ADC component may represent more serous fluid in a tuberculous cold abscess than in viscous pus formation. Routine surgery for spinal tuberculosis is not advocated. When necessary, the combined anterior and posterior approaches have been reported to be superior in lumbar and multilevel thoracic disease.^{42,43}

Brucellosis is an important endemic infection commonly seen in Mediterranean countries. Spinal involvement may simulate tuberculosis but often involves the lumbar spine.⁴⁴

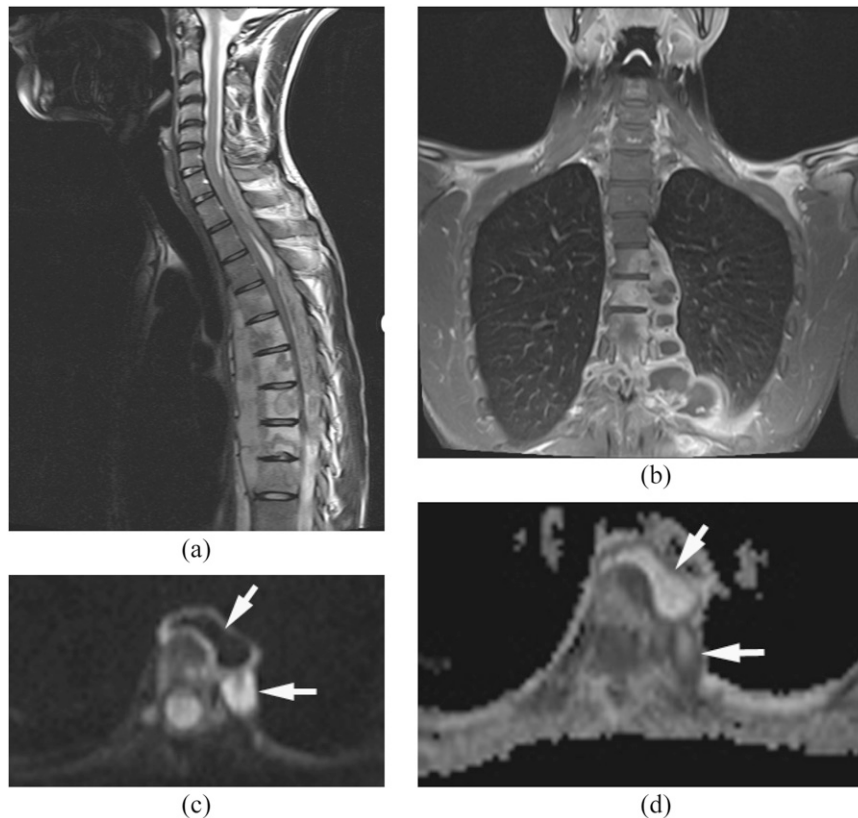
Fungal spinal infections include candidiasis (Figure 7), aspergillosis, blastomycosis, cryptococcosis, *Sporothrix*, histoplasmosis and coccidioidomycosis.^{1,2,16,38,41} Positive blood and tissue cultures are helpful in establishing the diagnosis but causative

organisms are not proven in a significant number of cases. Therapy is often delayed because of the difficulty in making the diagnosis. The imaging findings of most fungal spinal infections are non-specific. Vertebral body involvement with destruction can occur mimicking tuberculosis. Absence of T_2 high signal in adjacent discs is suggestive of fungal spondylitis.^{9,47} *Candida* spondylitis may be a simultaneous occurrence or late manifestation of hematogenously disseminated candidiasis. The most common location of *Candida* spondylitis is the lumbar spine. The formation of epidural abscess is uncommon.⁴⁶ Echinococcosis, onchocercosis, toxoplasmosis and toxocarosis can involve the spine.^{1,48}

MIMICS OF EPIDURAL AND PARASPINAL ABSCESES AND PUS COLLECTION

Disc herniation is extremely common and the diagnosis on MRI is usually straightforward. However, isolated epidural abscess (Figure 3) can be similar to extruded or sequestered disc herniation on MRI. DWI demonstrates facilitated diffusion in disc herniation while diffusion is restricted in an abscess. Epidural/subdural haematoma (Figure 8) and subarachnoid haemorrhage can show hyperintensity on DWI in the late subacute to early chronic phase and in the hyperacute phase. T_1 weighted images usually show hyperintensity in the late subacute haematoma due

Figure 6. Tuberculosis. Epidural abscess and paraspinal abscesses with spondylodiscitis. Tuberculosis was proven by surgical drainage. (a, b) Sagittal T_2 weighted image (a) and axial (b) post-contrast T_1 weighted images with fat saturation show osteomyelitis from T4 through T9 with subligamentous extension, epidural abscess and paraspinal abscesses. The discs are relatively spared. (c, d) Diffusion-weighted imaging (c) demonstrates partially hyper- and partially hypointensity with high and low apparent diffusion coefficient (ADC) values (arrows) (d). The high ADC component represents serous fluid in a cold abscess.



to methaemoglobin and can thus differentiate haematoma from abscess. However, the chronic phase of haematoma can show T_1 iso- to hypointensity with restricted diffusion due to the high viscosity containing hemichrome. CSF leaks can dissect through the epidural space associated with venous plexus engorgement and may appear similar to epidural abscess. However, DWI shows facilitated diffusion in the CSF collection in the epidural space and the venous plexus (Figure 9). Intraspinal epidermoid can have restricted diffusion that can mimic infection (Figure 10). Post-surgical wound infection (pus collection) has restricted diffusion while post-surgical fluid collection has facilitated diffusion (Figure 11). However, post-surgical haematoma can have restricted diffusion with well-defined round shape at the post-surgical site (Figure 12).

LIMITATION AND PITFALLS ON DIFFUSION-WEIGHTED IMAGING AND APPARENT DIFFUSION COEFFICIENT MAPS

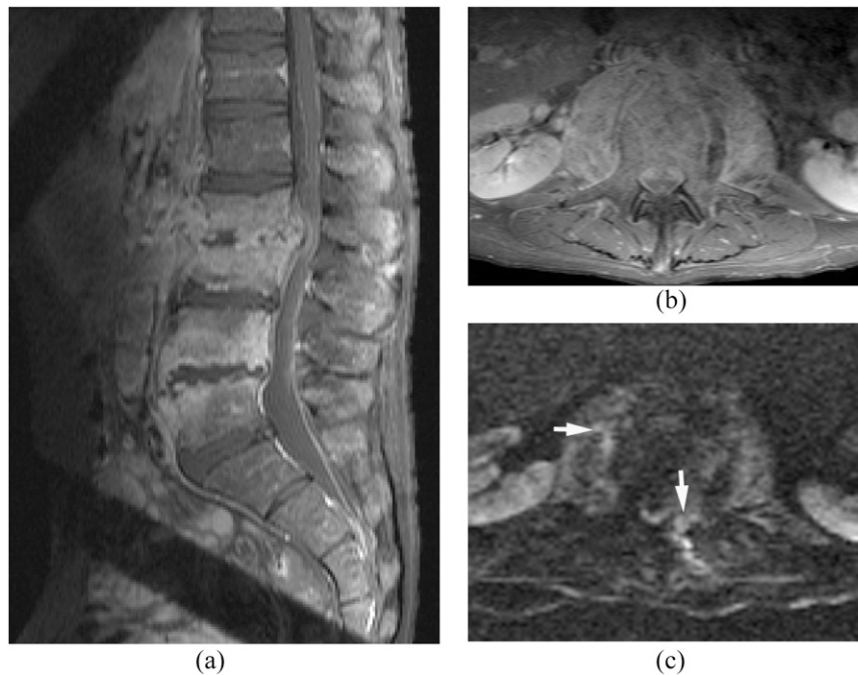
Many kinds of echoplanar imaging (EPI) and non-EPI diffusion sequences with various b -values have been reported in the diagnosis of spine and spinal cord disease.^{49–51} We routinely use spin-echo-type single-shot EPI sequence with parallel imaging techniques in our spine protocols because of the general availability and short acquisition time. For the detection and differentiation of abscesses or pus collections, we use a b -value of

0 and 1000 s mm^{-2} with the ADC map. DWI with lower b -value can show the CSF as partially high signal intensity due to the intravoxel incoherent motion and T_2 effect (Figure 13).⁵² To acquire less distortion diffusion-weighted images with the appropriate diffusion weighting, we use a parallel imaging factor of two.

Since DWI is typically implemented with EPI with fat saturation, there are many artefacts (susceptibility artefact, incomplete fat suppression, N/2 ghosting artefact, eddy current artefact and motion artefact) and imaging pitfalls on DWI and the ADC map. Paramagnetic susceptibility artefacts from surgical metallic devices cause significant image distortion on DWI (Figure 14). Incomplete fat saturation also occurs related to paramagnetic and diamagnetic susceptibility artefacts (Figure 1).

DWI usually shows hyperintensity in epidural and paraspinal abscesses associated with significantly lower ADC values than those in CSF collections, post-operative fluid collections and muscles. However, ADC maps sometimes show mixed intensity and slightly higher values than those reported in brain abscesses (Figure 2). Mixed intensity and slightly higher ADC values have been reported in subdural, epidural abscess, purulent meningitis and abdominopelvic abscesses than those in brain abscesses. The higher ADC values may be affected by prior antibiotic treatment,

Figure 7. Candidiasis. Epidural and psoas infections with spondylodiscitis. *Candida* was proven by biopsy. (a, b) Sagittal (a) and axial (b) post-contrast T_1 weighted image with fat saturation show spondylodiscitis at L2/3 and L4/5 with enhancing psoas and epidural lesions. (c) Diffusion-weighted imaging demonstrates hyperintensity in the epidural and psoas lesions suggestive of small pus collections (arrows).



or may be diluted by exudates, CSF or other fluid.^{6–8,53} If the abscess or pus collection is small, the ADC values can result in errors due to volume-averaging.

DWI has limited usefulness for the evaluation of vertebral body and disc. DWI usually shows slightly high signal intensity with increased ADC in vertebral osteomyelitis (Figure 15). Pathologically, the signal abnormality corresponds to bone marrow necrosis and oedema with inflammatory cell infiltration. ADC values of the bone marrow in spinal infection have been reported as significantly higher than those in malignancy. However, an overlap of ADC values is noted.^{9,54–56} DWI signals and the ADC values of the vertebral body are variable depending on the proportion between red and yellow bone marrow associated with ageing, degenerative changes and other conditions.^{51,57} The bone marrow fat (yellow bone marrow) causes signal void on DWI because DWI typically uses chemical fat

saturation techniques. Moreover, bony trabeculae cause signal loss related to diamagnetic susceptibility artefacts. Thus, the calculated ADC values are affected by the chemical fat saturation and susceptibility artefacts. DWI signals and ADC values of the disc can also be different owing to the variable presence of water contents with ageing and degenerative changes.

CONCLUSIONS

DWI with ADC maps is useful in early and accurate diagnosis of spinal and paraspinal infections, treatment planning and pre-operative assessment for surgical drainage and biopsy. Important differential diagnoses include epidural subdural or subarachnoid haemorrhage, CSF leak, disc herniation, synovial cyst, granulation tissue, intra- or extradural tumour and post-surgical fluid collections. Recognition of artefacts on DWI and ADC maps is essential when interpreting DWI of spinal and paraspinal infections.

REFERENCES

1. Tali ET. Spinal infections. *Eur J Radiol* 2004; **50**: 120–33. doi: [10.1016/j.ejrad.2003.10.022](https://doi.org/10.1016/j.ejrad.2003.10.022)
2. Darouiche RO. Spinal epidural abscess. *N Engl J Med* 2006; **355**: 2012–20. doi: [10.1056/NEJMr055111](https://doi.org/10.1056/NEJMr055111)
3. Kourbeti IS, Tsiodras S, Boumpas DT. Spinal infections: evolving concepts. *Curr Opin Rheumatol* 2008; **20**: 471–9. doi: [10.1097/BOR.0b013e3282ff5e66](https://doi.org/10.1097/BOR.0b013e3282ff5e66)
4. Tins BJ, Cassar-Pullicino VN. MR imaging of spinal infection. *Semin Musculoskelet Radiol* 2004; **8**: 215–29. doi: [10.1055/s-2004-835362](https://doi.org/10.1055/s-2004-835362)
5. Fertikh D, Krejza J, Cunqueiro A, Danish S, Alokaili R, Melhem ER. Discrimination of capsular stage brain abscesses from necrotic or cystic neoplasms using diffusion-weighted magnetic resonance imaging. *J Neurosurg* 2007; **106**: 76–81. doi: [10.3171/jns.2007.106.1.76](https://doi.org/10.3171/jns.2007.106.1.76)
6. Ferreira NP, Otta GM, do Amaral LL, da Rocha AJ. Imaging aspects of pyogenic infections of the central nervous system. *Top Magn Reson Imaging* 2005; **16**: 145–54.
7. Abe M, Takayama Y, Yamashita H, Noguchi M, Sagoh T. Purulent meningitis with

- unusual diffusion-weighted MRI findings. *Eur J Radiol* 2002; **44**: 1–4.
8. Tsuchiya K, Osawa A, Katase S, Fujikawa A, Hachiya J, Aoki S. Diffusion-weighted MRI of subdural and epidural empyemas. *Neuroradiology* 2003; **45**: 220–3. doi: [10.1007/s00234-003-0949-5](https://doi.org/10.1007/s00234-003-0949-5)
 9. Thurnher MM, Bammer R. Diffusion-weighted magnetic resonance imaging of the spine and spinal cord. *Semin Roentgenol* 2006; **41**: 294–311. doi: [10.1053/j.ro.2006.07.003](https://doi.org/10.1053/j.ro.2006.07.003)
 10. Eastwood JD, Vollmer RT, Provenzale JM. Diffusion-weighted imaging in a patient with vertebral and epidural abscesses. *AJNR Am J Neuroradiol* 2002; **23**: 496–8.
 11. Trombly R, Guest JD. Acute central cord syndrome arising from a cervical epidural abscess: case report. *Neurosurgery* 2007; **61**: E424–5. doi: [10.1227/01.NEU.0000255515.12085.60](https://doi.org/10.1227/01.NEU.0000255515.12085.60)
 12. Palestro CJ, Love C, Miller TT. Infection and musculoskeletal conditions: imaging of musculoskeletal infections. *Best Pract Res Clin Rheumatol* 2006; **20**: 1197–218.
 13. Butler JS, Shelly MJ, Timlin M, Powderly WG, O'Byrne JM. Nontuberculous pyogenic spinal infection in adults: a 12-year experience from a tertiary referral center. *Spine (Phila Pa 1976)* 2006; **31**: 2695–700.
 14. Boden SD, Davis DO, Dina TS, Sunner JL, Wiesel SW. Postoperative diskitis: distinguishing early MR imaging findings from normal postoperative disk space changes. *Radiology* 1992; **184**: 765–71. doi: [10.1148/radiology.184.3.1509065](https://doi.org/10.1148/radiology.184.3.1509065)
 15. Modic MT, Feiglin DH, Piraino DW, Boumphey F, Weinstein MA, Duchesneau PM, et al. Vertebral osteomyelitis: assessment using MR. *Radiology* 1985; **157**: 157–66. doi: [10.1148/radiology.157.1.3875878](https://doi.org/10.1148/radiology.157.1.3875878)
 16. Lury K, Smith JK, Castillo M. Imaging of spinal infections. *Semin Roentgenol* 2006; **41**: 363–79. doi: [10.1053/j.ro.2006.07.008](https://doi.org/10.1053/j.ro.2006.07.008)
 17. Conaughty JM, Chen J, Martinez OV, Chiappetta G, Brookfield KE, Eismont FJ. Efficacy of linezolid versus vancomycin in the treatment of methicillin-resistant *Staphylococcus aureus* discitis: a controlled animal model. *Spine (Phila Pa 1976)* 2006; **31**: E830–2.
 18. Stevens QE, Seibly JM, Chen YH, Dickerman RD, Noel J, Kattner KA. Reactivation of dormant lumbar methicillin-resistant *Staphylococcus aureus* osteomyelitis after 12 years. *J Clin Neurosci* 2007; **14**: 585–9. doi: [10.1016/j.jocn.2005.12.006](https://doi.org/10.1016/j.jocn.2005.12.006)
 19. Mahboubi S, Morris MC. Imaging of spinal infections in children. *Radiol Clin North Am* 2001; **39**: 215–22.
 20. Bair-Merritt MH, Chung C, Collier A. Spinal epidural abscess in a young child. *Pediatrics* 2000; **106**: E39.
 21. Glazer PA, Hu SS. Pediatric spinal infections. *Orthop Clin North Am* 1996; **27**: 111–23.
 22. Wiley AM, Trueta J. The vascular anatomy of the spine and its relationship to pyogenic vertebral osteomyelitis. *J Bone Joint Surg Br* 1959; **41-B**: 796–809.
 23. Ozuna RM, Delamarter RB. Pyogenic vertebral osteomyelitis and postsurgical disc space infections. *Orthop Clin North Am* 1996; **27**: 87–94.
 24. Calderone RR, Larsen JM. Overview and classification of spinal infections. *Orthop Clin North Am* 1996; **27**: 1–8.
 25. Uchida K, Nakajima H, Yayama T, Sato R, Kobayashi S, Chen KB, et al. Epidural abscess associated with pyogenic spondylodiscitis of the lumbar spine; evaluation of a new MRI staging classification and imaging findings as indicators of surgical management: a retrospective study of 37 patients. *Arch Orthop Trauma Surg* 2010; **130**: 111–18.
 26. Solomou E, Maragkos M, Kotsarini C, Konstantinou D, Maraziotis T. Multiple spinal epidural abscesses extending to the whole spinal canal. *Magn Reson Imaging* 2004; **22**: 747–50. doi: [10.1016/j.mri.2004.01.072](https://doi.org/10.1016/j.mri.2004.01.072)
 27. Ghosh PS, Loddenkemper T, Blanco MB, Marks M, Sabella C, Ghosh D. Holocord spinal epidural abscess. *J Child Neurol* 2009; **24**: 768–71. doi: [10.1177/0883073808329524](https://doi.org/10.1177/0883073808329524)
 28. Ledermann HP, Schweitzer ME, Morrison WB, Carrino JA. MR imaging findings in spinal infections: rules or myths? *Radiology* 2003; **228**: 506–14. doi: [10.1148/radiol.2282020752](https://doi.org/10.1148/radiol.2282020752)
 29. Wagner SC, Schweitzer ME, Morrison WB, Przybylski GJ, Parker L. Can imaging findings help differentiate spinal neuropathic arthropathy from disk space infection? Initial experience. *Radiology* 2000; **214**: 693–9.
 30. Numaguchi Y, Rigamonti D, Rothman MI, Sato S, Mihara F, Sadato N. Spinal epidural abscess: evaluation with gadolinium-enhanced MR imaging. *Radiographics* 1993; **13**: 545–59. doi: [10.1148/radiographics.13.3.8316663](https://doi.org/10.1148/radiographics.13.3.8316663)
 31. Longo M, Granata F, Ricciardi K, Gaeta M, Blandino A. Contrast-enhanced MR imaging with fat suppression in adult-onset septic spondylodiscitis. *Eur Radiol* 2003; **13**: 626–37.
 32. Doita M, Nabeshima Y, Nishida K, Fujioka H, Kurosaka M. Septic arthritis of lumbar facet joints without predisposing infection. *J Spinal Disord Tech* 2007; **20**: 290–5. doi: [10.1097/01.bsd.0000211285.91271.b3](https://doi.org/10.1097/01.bsd.0000211285.91271.b3)
 33. Smida M, Lejri M, Kandara H, Sayed M, Ben Chehida F, Ben Ghachem M. Septic arthritis of a lumbar facet joint case report and review of the literature. *Acta Orthop Belg* 2004; **70**: 290–4.
 34. Mellado JM, Pérez del Palomar L, Camins A, Salvadó E, Ramos A, Saurí A. MR imaging of spinal infection: atypical features, interpretive pitfalls and potential mimickers. *Eur Radiol* 2004; **14**: 1980–9. doi: [10.1007/s00330-004-2310-8](https://doi.org/10.1007/s00330-004-2310-8)
 35. Muffoletto AJ, Ketonen LM, Mader JT, Crow WN, Hadjipavlou AG. Hematogenous pyogenic facet joint infection. *Spine (Phila Pa 1976)* 2001; **26**: 1570–6.
 36. Coscia ME, Trammell TR. Pyogenic lumbar facet joint arthritis with intradural extension: a case report. *J Spinal Disord Tech* 2002; **15**: 526–8.
 37. Velissaris D, Aretha D, Fligou F, Filos KS. Spinal subdural *Staphylococcus aureus* abscess: case report and review of the literature. *World J Emerg Surg* 2009; **4**: 31. doi: [10.1186/1749-7922-4-31](https://doi.org/10.1186/1749-7922-4-31)
 38. Reihnsaus E, Waldbaur H, Seeling W. Spinal epidural abscess: a meta-analysis of 915 patients. *Neurosurg Rev* 2000; **23**: 175–204.
 39. Dörflinger-Hejlek E, Kirsch EC, Reiter H, Opravil M, Kaim AH. Diffusion-weighted MR imaging of intramedullary spinal cord abscess. *AJNR Am J Neuroradiol* 2010; **31**: 1651–2.
 40. Harada Y, Tokuda O, Matsunaga N. Magnetic resonance imaging characteristics of tuberculous spondylitis vs. pyogenic spondylitis. *Clin Imaging* 2008; **32**: 303–9. doi: [10.1016/j.clinimag.2007.03.015](https://doi.org/10.1016/j.clinimag.2007.03.015)
 41. Skaf GS, Kanafani ZA, Araj GF, Kanj SS. Non-pyogenic infections of the spine. *Int J Antimicrob Agents* 2010; **36**: 99–105. doi: [10.1016/j.ijantimicag.2010.03.023](https://doi.org/10.1016/j.ijantimicag.2010.03.023)
 42. Karaeminogullari O, Aydinli U, Ozerdemoglu R, Ozturk C. Tuberculosis of the lumbar spine: outcomes after combined treatment of two-drug therapy and surgery. *Orthopedics* 2007; **30**: 55–9.
 43. Zhang HQ, Guo CF, Xiao XG, Long WR, Deng ZS, Chen J. One-stage surgical management for multilevel tuberculous spondylitis of the upper thoracic region by anterior decompression, strut autografting, posterior instrumentation, and fusion. *J Spinal Disord Tech* 2007; **20**: 263–7.
 44. Oztekin O, Calli C, Adibelli Z, Kitis O, Eren C, Altinok T. Brucellar spondylodiscitis: magnetic resonance imaging features with conventional sequences and diffusion-weighted imaging. *Radiol Med* 2010; **115**: 794–803. doi: [10.1007/s11547-010-0530-3](https://doi.org/10.1007/s11547-010-0530-3)
 45. Chia SL, Tan BH, Tan CT, Tan SB. *Candida* spondylodiscitis and epidural abscess:

- management with shorter courses of anti-fungal therapy in combination with surgical debridement. *J Infect* 2005; **51**: 17–23.
46. Aganovic L, Hoda RS, Rumboldt Z. Hyperintensity of spinal *Cryptococcus* infection on diffusion-weighted MR images. *AJR Am J Roentgenol* 2004; **183**: 1176–7. doi: [10.2214/ajr.183.4.1831176](https://doi.org/10.2214/ajr.183.4.1831176)
47. Williams RL, Fukui MB, Meltzer CC, Swarnkar A, Johnson DW, Welch W. Fungal spinal osteomyelitis in the immunocompromised patient: MR findings in three cases. *AJNR Am J Neuroradiol* 1999; **20**: 381–5.
48. Akhan O, Dinçer A, Saatçi I, Gülekon N, Besim A. Spinal intradural hydatid cyst in a child. *Br J Radiol* 1991; **64**: 465–6.
49. Andre JB, Bammer R. Advanced diffusion-weighted magnetic resonance imaging techniques of the human spinal cord. *Top Magn Reson Imaging* 2010; **21**: 367–78. doi: [10.1097/RMR.0b013e31823e65a1](https://doi.org/10.1097/RMR.0b013e31823e65a1)
50. Hori M, Okubo T, Aoki S, Kumagai H, Araki T. Line scan diffusion tensor MRI at low magnetic field strength: feasibility study of cervical spondylotic myelopathy in an early clinical stage. *J Magn Reson Imaging* 2006; **23**: 183–8.
51. Raya JG, Dietrich O, Reiser MF, Baur-Melnyk A. Methods and applications of diffusion imaging of vertebral bone marrow. *J Magn Reson Imaging* 2006; **24**: 1207–20. doi: [10.1002/jmri.20748](https://doi.org/10.1002/jmri.20748)
52. Le Bihan D, Breton E, Lallemand D, Grenier P, Cabanis E, Laval-Jeantet M. MR imaging of intravoxel incoherent motions: application to diffusion and perfusion in neurologic disorders. *Radiology* 1986; **161**: 401–7. doi: [10.1148/radiology.161.2.3763909](https://doi.org/10.1148/radiology.161.2.3763909)
53. Oto A, Schmid-Tannwald C, Agrawal G, Kayhan A, Lakadamyali H, Orrin S, et al. Diffusion-weighted MR imaging of abdominopelvic abscesses. *Emerg Radiol* 2011; **18**: 515–24. doi: [10.1007/s10140-011-0976-1](https://doi.org/10.1007/s10140-011-0976-1)
54. Castillo M, Arbelaez A, Smith K, Fisher LL. Diffusion-weighted MR imaging offers no advantage over routine noncontrast MR imaging in the detection of vertebral metastases. *AJNR Am J Neuroradiol* 2000; **21**: 948–53.
55. Pui MH, Mitha A, Rae WI, Corr P. Diffusion-weighted magnetic resonance imaging of spinal infection and malignancy. *J Neuroimaging* 2005; **15**: 164–70.
56. Herneth AM, Friedrich K, Weidekamm C, Schibany N, Krestan C, Czerny C, et al. Diffusion weighted imaging of bone marrow pathologies. *Eur J Radiol* 2005; **55**: 74–83. doi: [10.1016/j.ejrad.2005.03.031](https://doi.org/10.1016/j.ejrad.2005.03.031)
57. Padhani AR, van Ree K, Collins DJ, D'Sa S, Makris A. Assessing the relation between bone marrow signal intensity and apparent diffusion coefficient in diffusion-weighted MRI. *AJR Am J Roentgenol* 2013; **200**: 163–70. doi: [10.2214/AJR.11.8185](https://doi.org/10.2214/AJR.11.8185)

Figure 8. Epidural haematoma after trauma. (a, b) Sagittal T_2 (a) and T_1 weighted images (b) show hyperintense epidural haematoma from T2 through T6 posteriorly. (c) Diffusion-weighted imaging demonstrates hyperintensity in the epidural haematoma (arrow) similar to an epidural abscess.

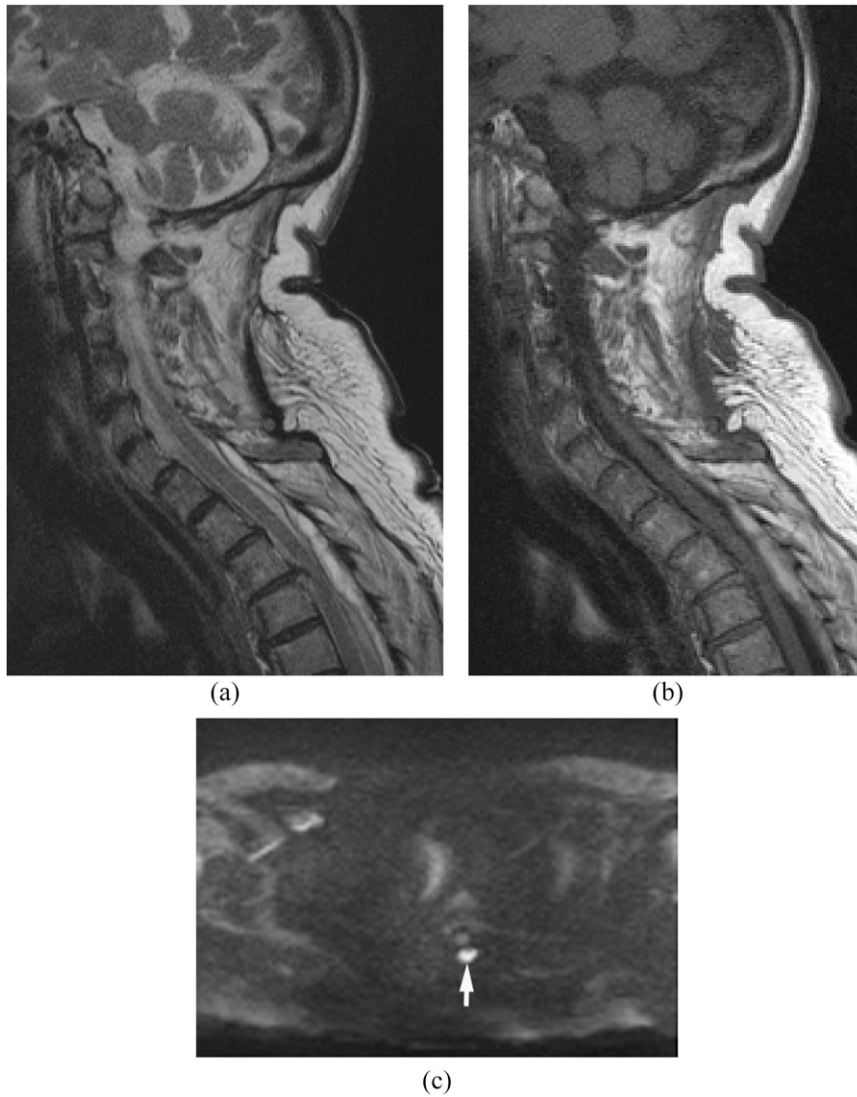


Figure 9. Cerebrospinal fluid leak after lumbar puncture in an infant. (a) Sagittal T_2 weighted image shows hyperintensity in the posterior epidural space extending through the whole spine. (b) Axial post-contrast T_1 weighted image with fat saturation shows epidural enhancement due to the prominent venous plexus. (c) Diffusion-weighted imaging demonstrates hypointensity in the posterior epidural space (arrow).

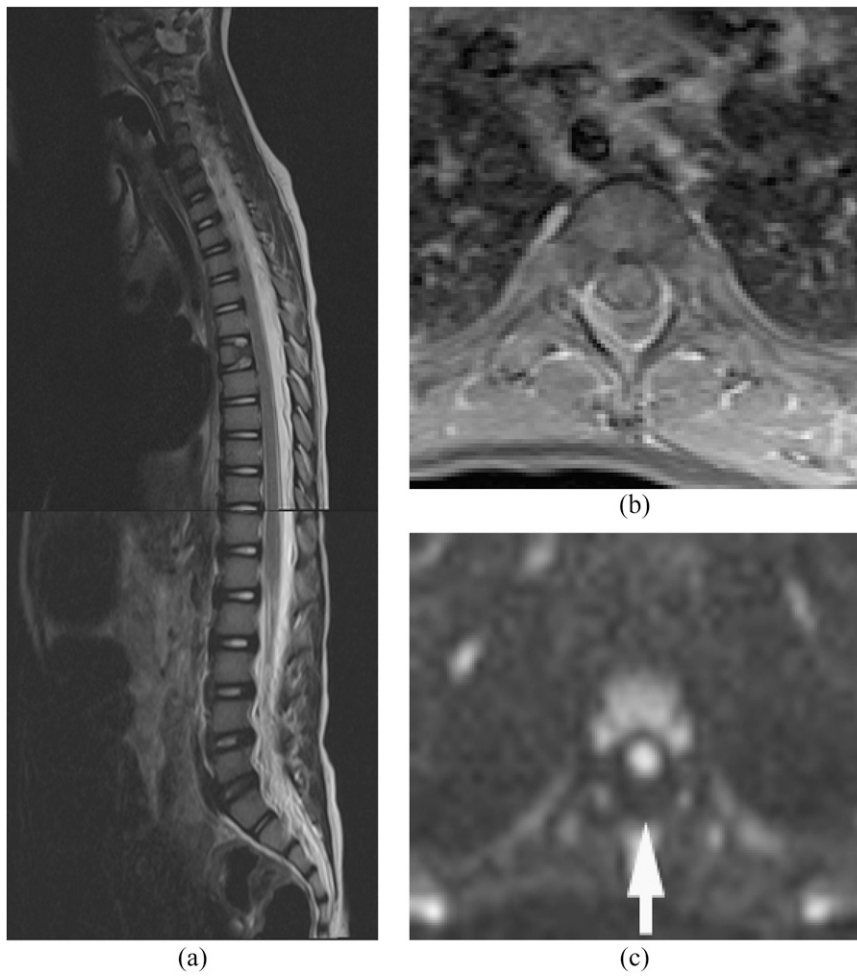


Figure 10. Ruptured epidermoid with chemical meningitis. (a, b) Sagittal MRI shows a large T_2 hypointense (a) and T_1 hyperintense (b) mass with posterior scalloping of the vertebral bodies. (c) Diffusion-weighted imaging demonstrates slight hyperintensity (not shown) in the mass with decreased apparent diffusion coefficient (arrow).



Figure 11. Post-operative fluid collection. (a) Axial post-contrast T_1 weighted image with fat saturation shows fluid collections at the post-operative site with peripheral enhancement. (b, c) Diffusion-weighted imaging shows the fluid collections as hypointense (b) associated with increased apparent diffusion coefficient (c) consistent with seroma or pseudomeningocele (arrows).

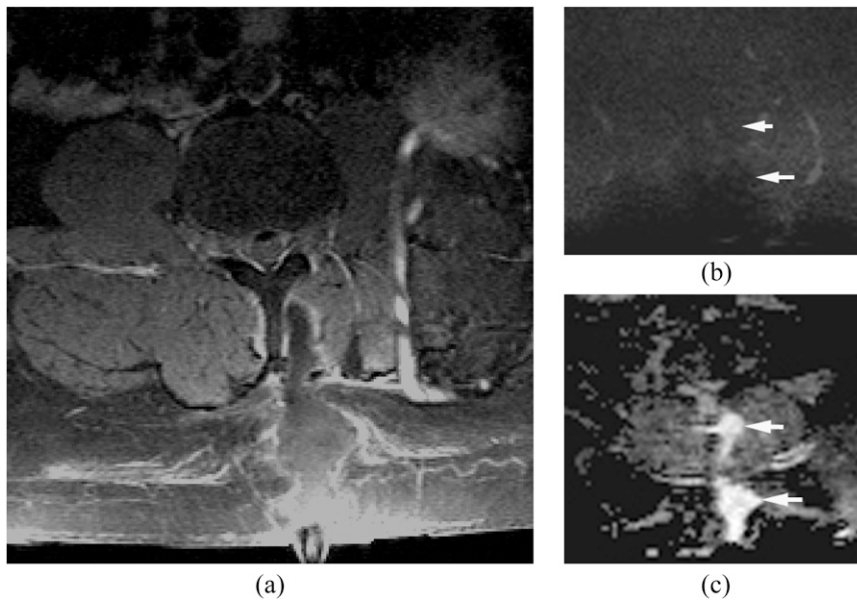


Figure 12. Post-operative haematoma. (a, b) Sagittal T_2 (a) and T_1 weighted images (b) show a hyperintense round lesion at the post-operative site. (c) Diffusion-weighted imaging shows hyperintense signal in the lesion (arrow) with decreased apparent diffusion coefficient (not shown) similar to an abscess. A few white blood cells with blood products were proven by drainage.

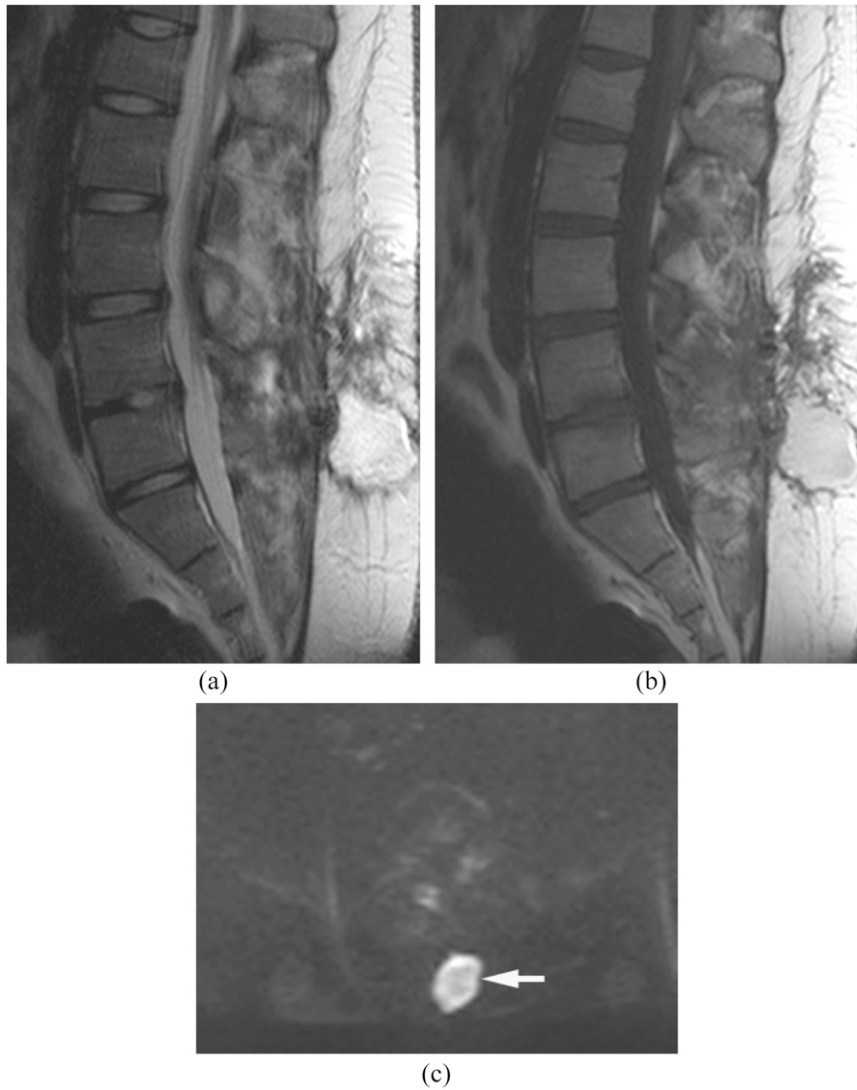
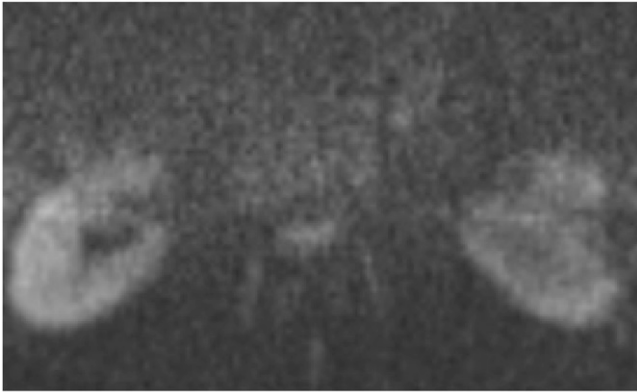
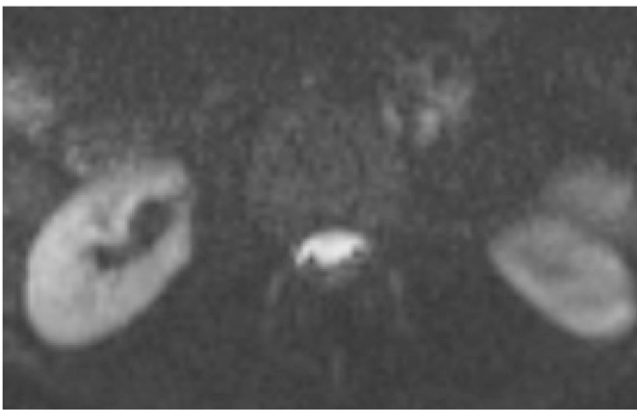


Figure 13. Diffusion-weighted imaging (DWI) with b -values of 500 vs 1000 s mm^{-2} . (a) We routinely use DWI in spine protocols with a b -value of 1000 s mm^{-2} for the evaluation of abscess and pus collection. (b) DWI with a b -value of 500 s mm^{-2} shows partially hyperintense normal cerebrospinal fluid in the spinal canal, which is difficult to differentiate from pus collection. DWI use with low or intermediate b -value is not adequate for this purpose since the signal is more influenced by T_2 effect and intravoxel incoherent motion.



(a)



(b)

Figure 14. Susceptibility artefacts. (a, b) Sagittal (a) and axial (b) T_2 weighted images show a hyperintense lesion in the epidural space posterolaterally (arrows) with relatively mild susceptibility artefacts from a fusion device. (c) Axial post-contrast T_1 weighted image with fat saturation is difficult to detect the epidural abscess owing to motion artefacts. (d) Diffusion-weighted imaging shows no apparent hyperintensity suggestive of the epidural abscess owing to susceptibility artefacts from the fusion device.

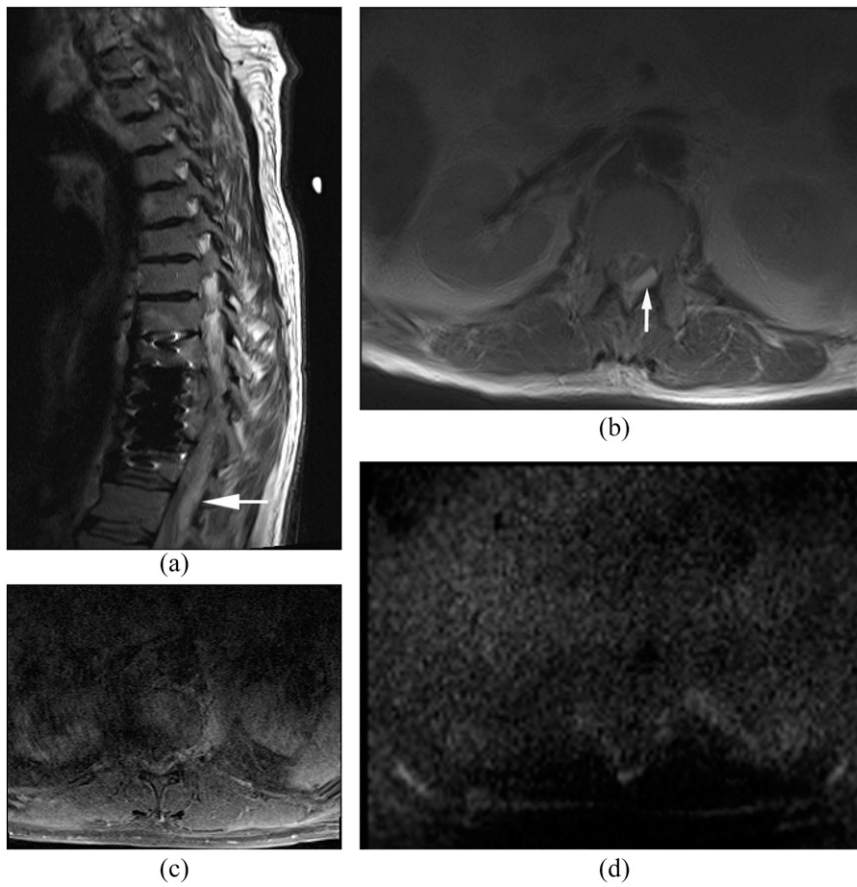


Figure 15. Vertebral osteomyelitis. (a) Sagittal post-contrast T_1 weighted image with fat saturation shows enhancement in the disc and vertebral bodies at L4 and L5 consistent with discitis/osteomyelitis. (b, c) There is mild hyperintensity on diffusion-weighted imaging (b) with increased apparent diffusion coefficient (c) in the adjacent bone marrow. (d) Pathology demonstrates extensive bone necrosis and oedema with patchy inflammatory cell infiltrations.

